Figure 1: Bias and standard deviation of the apparent surface temperature as a function of surface wind speed between two models for all profiles of the GARAND26 data set. The channel numbers 1 to 8 refer to the SSM/I channels and are as follows: (1) 19 GHz V, (2) 19 GHz H, (3) 22 GHz V, (4) 22 GHz H, (5) 37 GHz V, (6) 37 GHz H, (7) 85 GHz V and (8) 85 GHz H. The satellite view angle with respect to nadir is 44.93°. This corresponds to an earth incidence angle of 53°. Model definitions are summarized in Table 2. 1dvar2 parameter choices are defined in Table 1b. The top bar plots compare models 1dvar0 and 1dvar2 (#2) to evaluate the impact of the isothermal atmosphere approximation. The bottom bar plots compare 1dvar2 (#1) and 1dvar2 (#3) to study the impact of the choice for handling the multiple reflection in the 1dvar2 model.
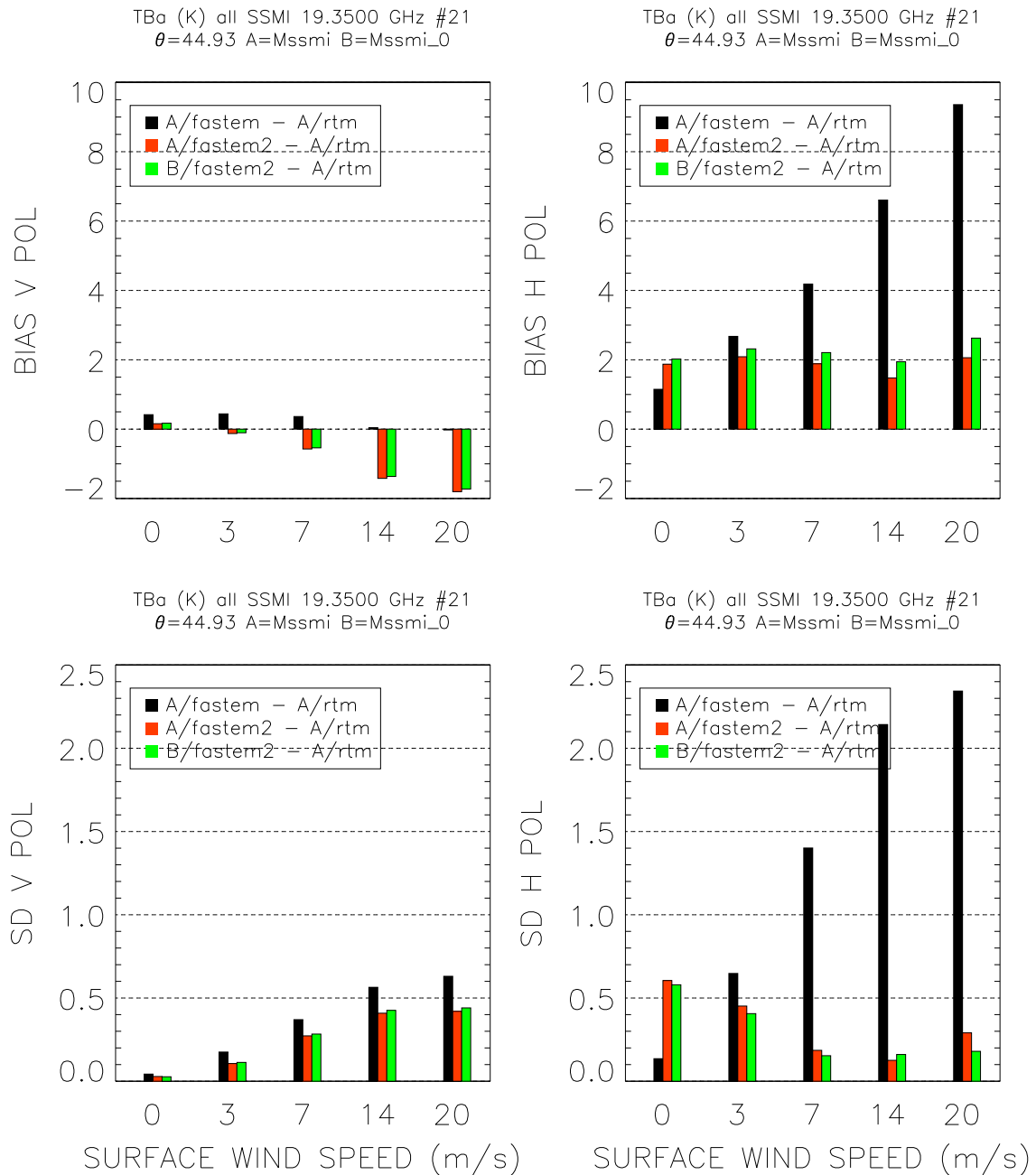
Figure 2a: Bias and standard deviation of the apparent surface temperature at the SSM/I frequency of 19.35 GHz as a function of surface wind speed for 3 sets of model intercomparisons for all profiles of the GARAND26 data set. Model definitions are summarized in Table 2. The intercomparison sets are as follows: Set 1: fastem -rtm (black or first bar), Set 2: fastem2-rtm(red or second bar) and Set 3: fastem2 simplified (Section 6.3) - rtm (green or third bar).
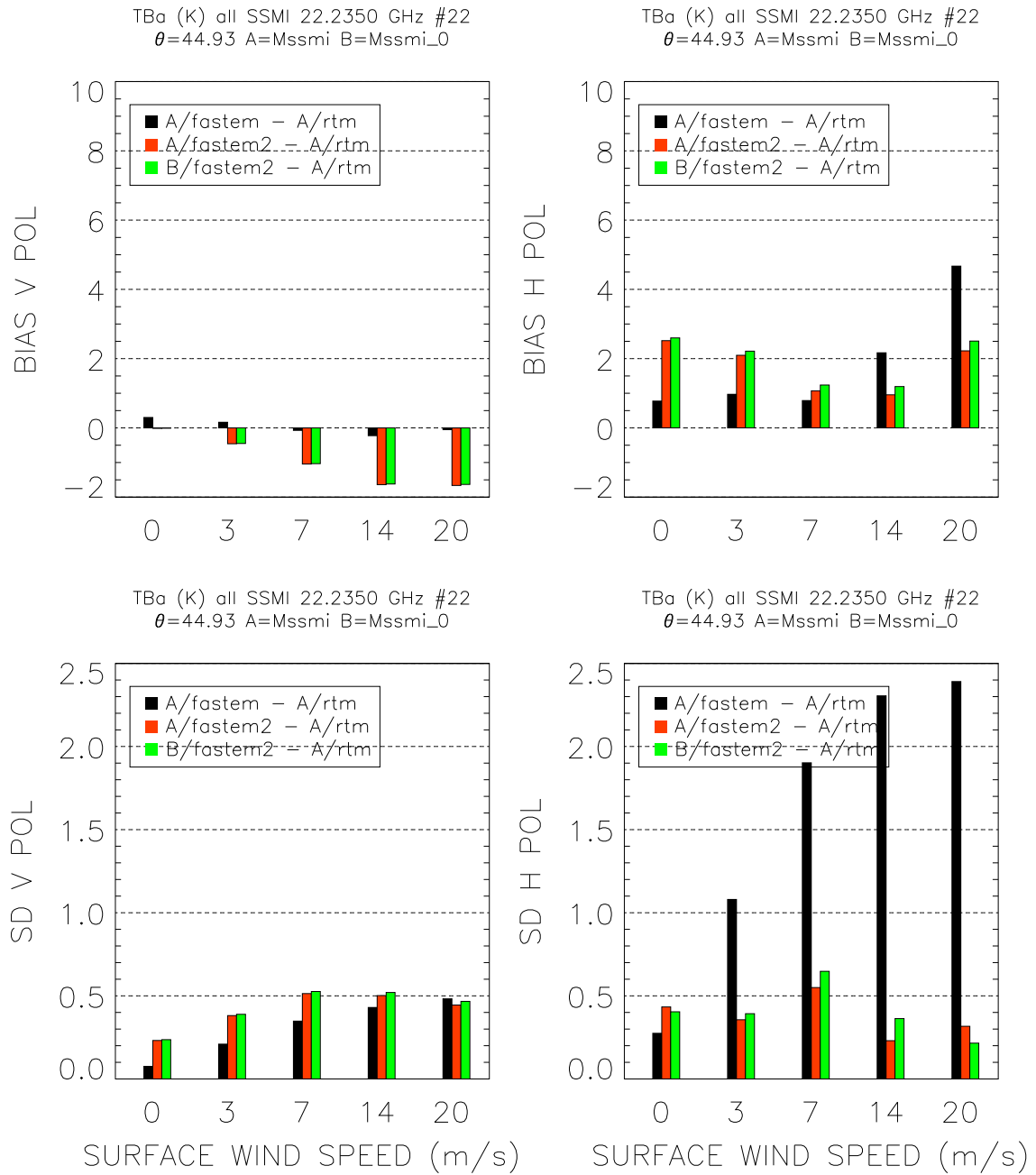
Figure 2b: Same as Figure 2a but for the SSM/I frequency of 22.235 GHz.
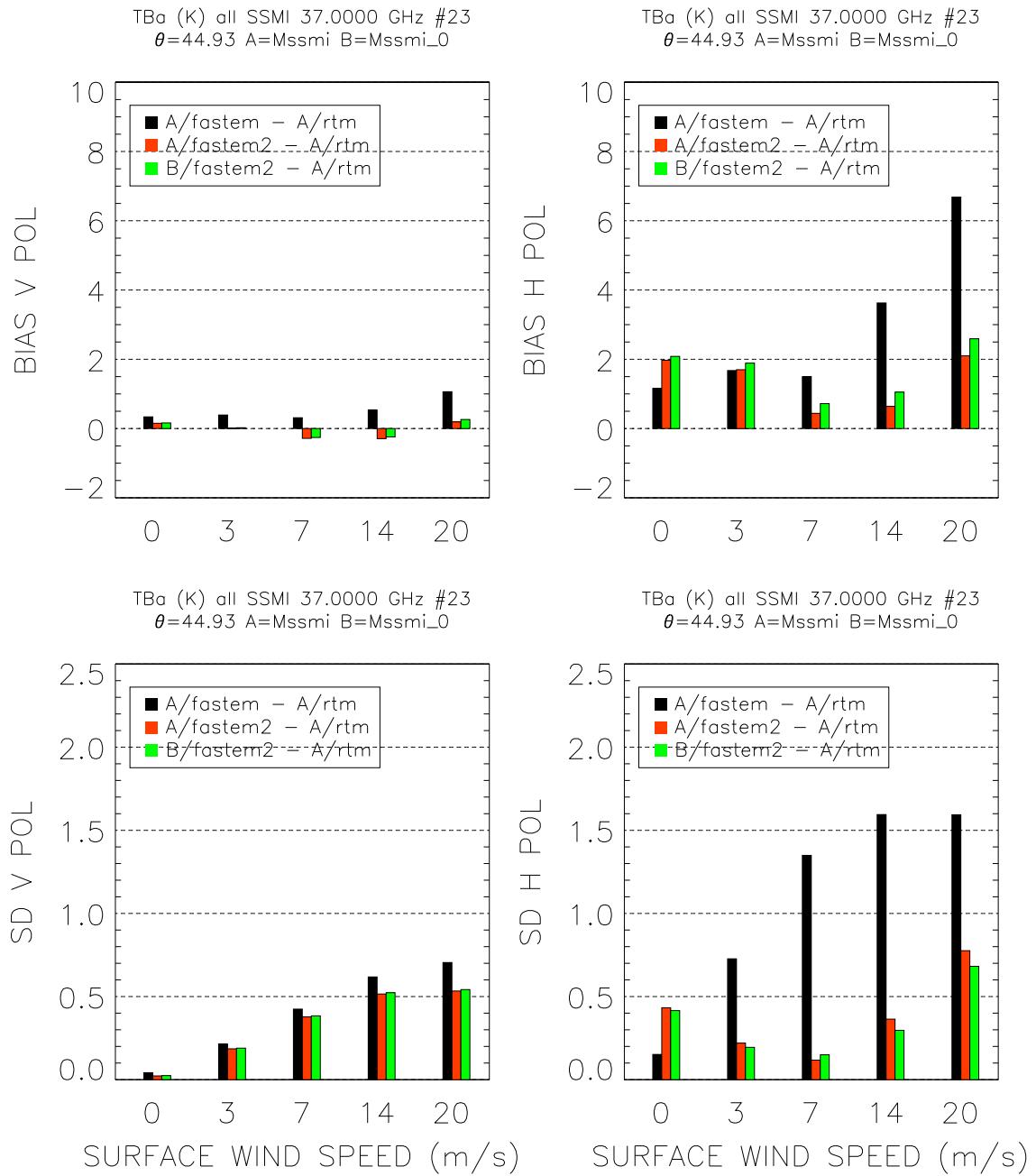
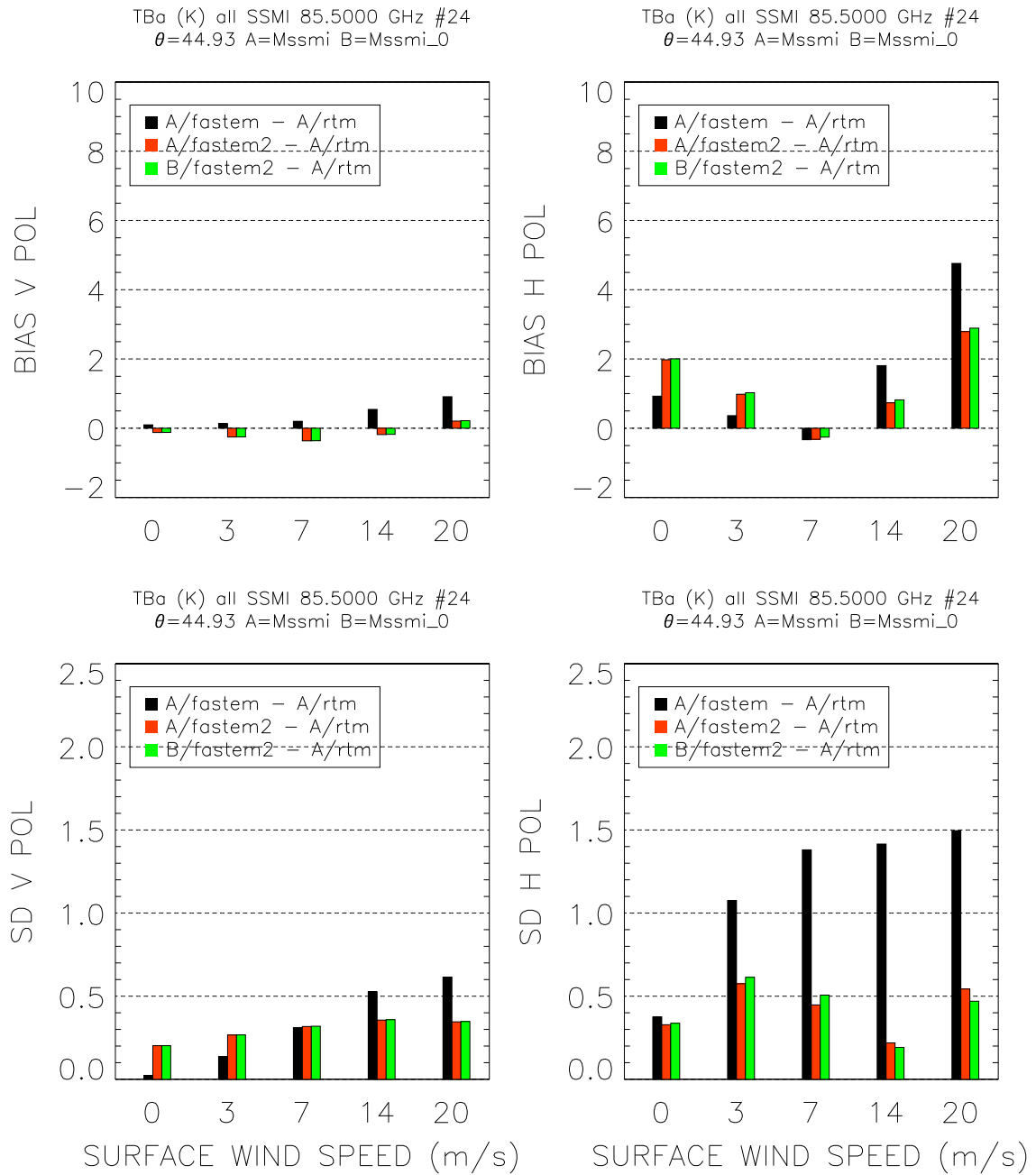Figure 2c: Same as Figure 2a but for the SSM/I frequency of 37.0 GHz.

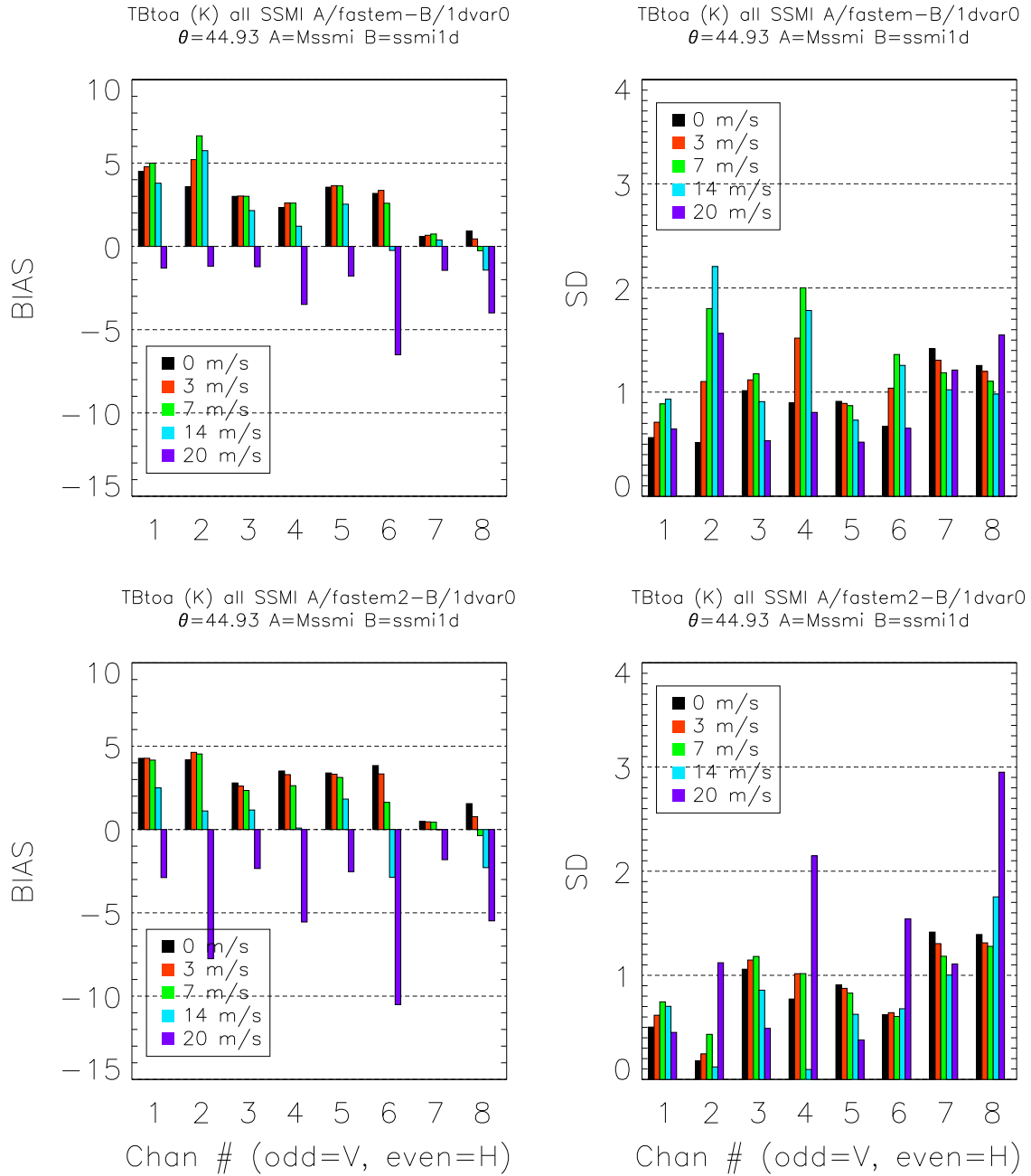Figure 2d: Same as Figure 2a but for the SSM/I frequency of 85.5 GHz.

Figure 3: Bias and standard deviation of the brightness temperature at the top of the atmosphere as a function of surface wind speed between two models for all profiles of the GARAND26 data set. The channel numbers 1 to 8 refer to the SSM/I channels and are as follows: (1) 19 GHz V, (2) 19 GHz H, (3) 22 GHz V, (4) 22 GHz H, (5) 37 GHz V, (6) 37 GHz H, (7) 85 Ghz V and (8) 85 GHz H. The satellite view angle with respect to nadir is 44.93°. The top bar plots compare models fastem and 1dvar0, the bottom bar plots compare models fastem2 and 1dvar0. Model definitions are summarized in Table 2.
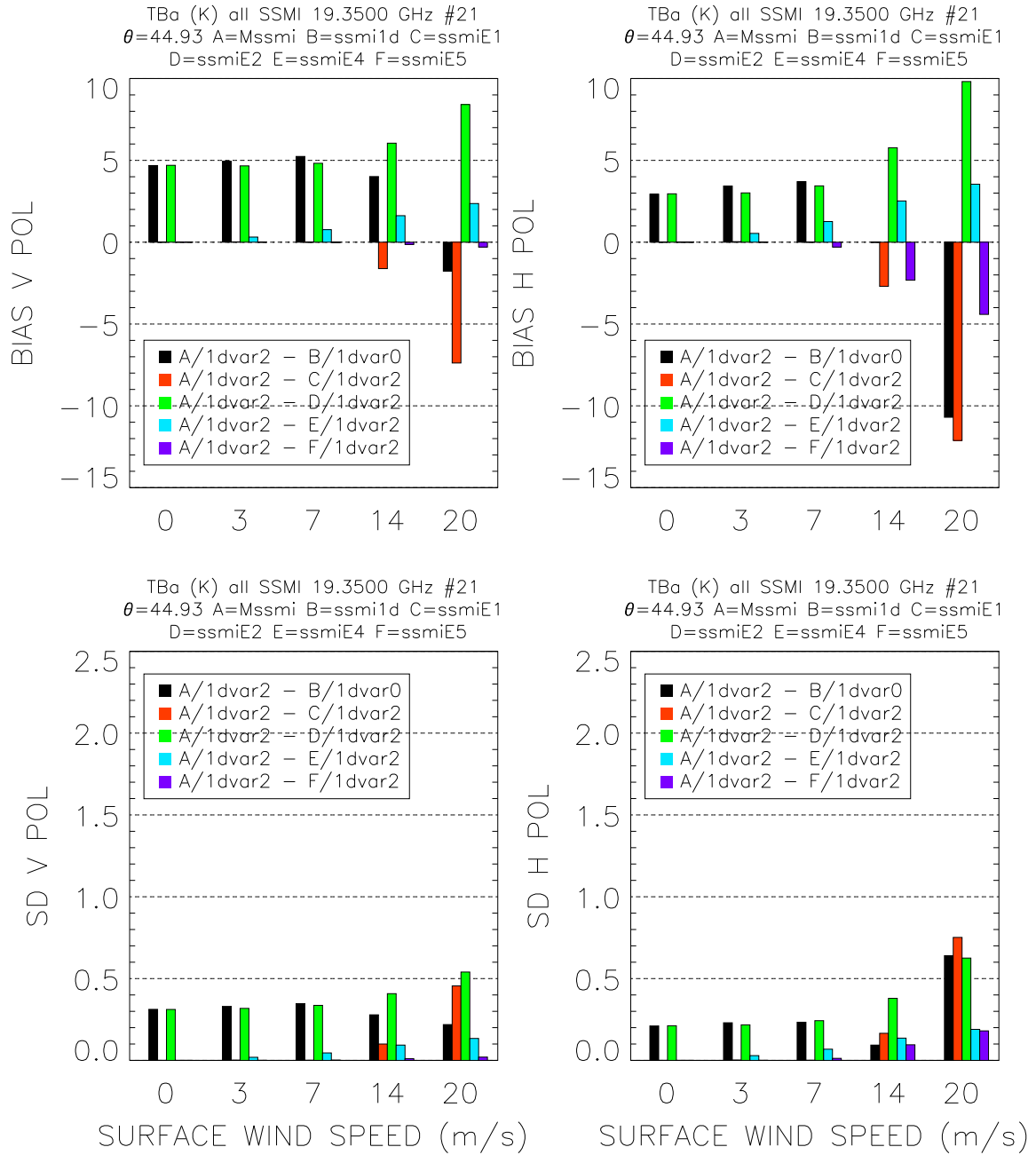
Figure 4a: Bias and standard deviation of the apparent surface temperature at the SSM/I frequency of 19.35 GHz as a function of surface wind speed for 5 sets of model intercomparisons for all profiles of the GARAND26 data set. The differencess were performed to test the impact of parameter changes. Model definitions are summarized in Table 2. 1dvar2 parameter selections are defined in Table 1b. The intercomparison sets are as follows: Set 1: 1dvar2(#1)-1dvar0, Set 2: 1dvar2(#1)-1dvar2(#4)—foam change, Set 3: 1dvar2(#1)-1dvar2(#5)—dielectric constant change, Set 4: 1dvar2(#1)-1dvar2(#6)—Bragg scattering change, Set 5: 1dvar2(#1)-1dvar2(#3)—multiple scattering change.
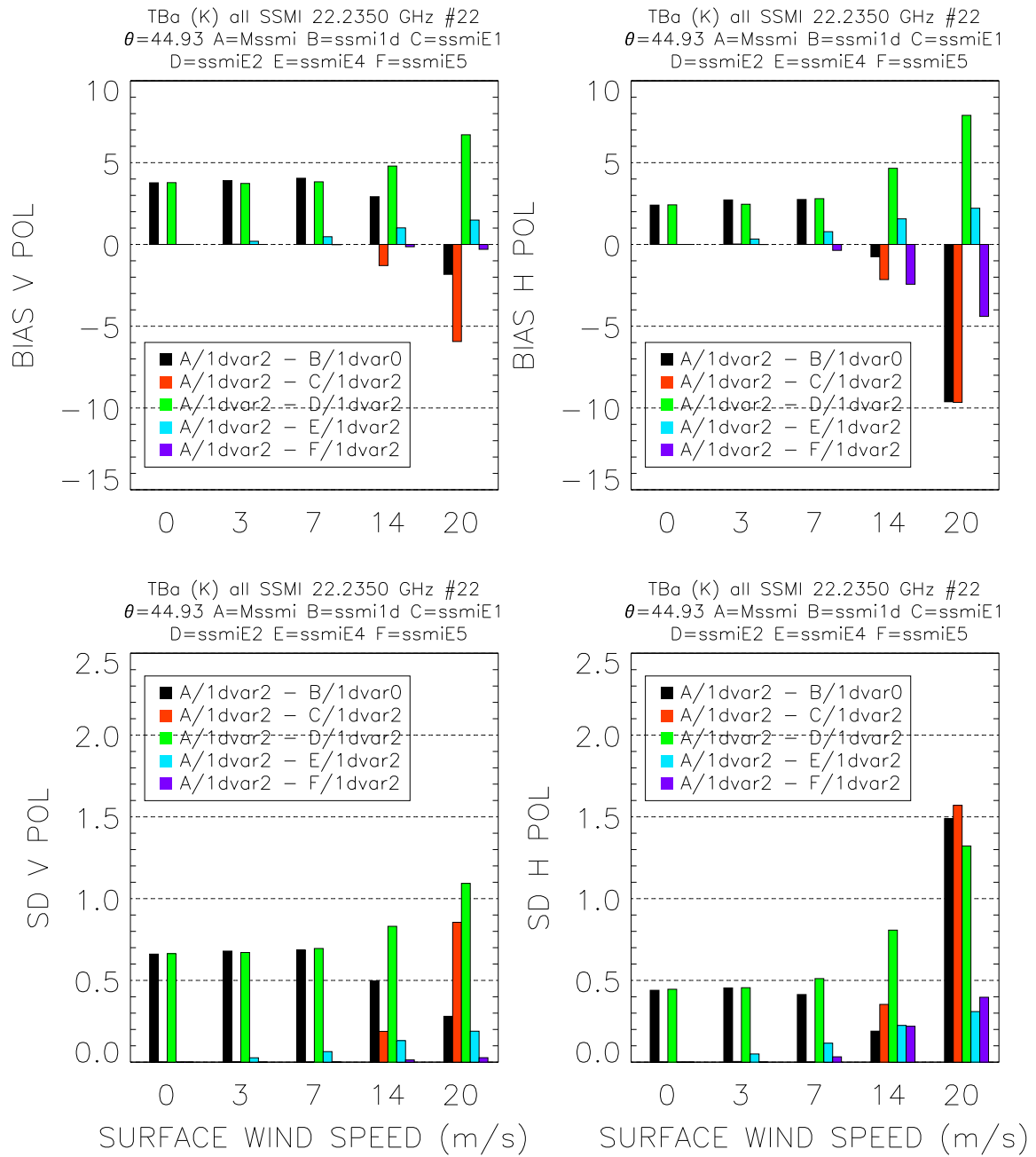
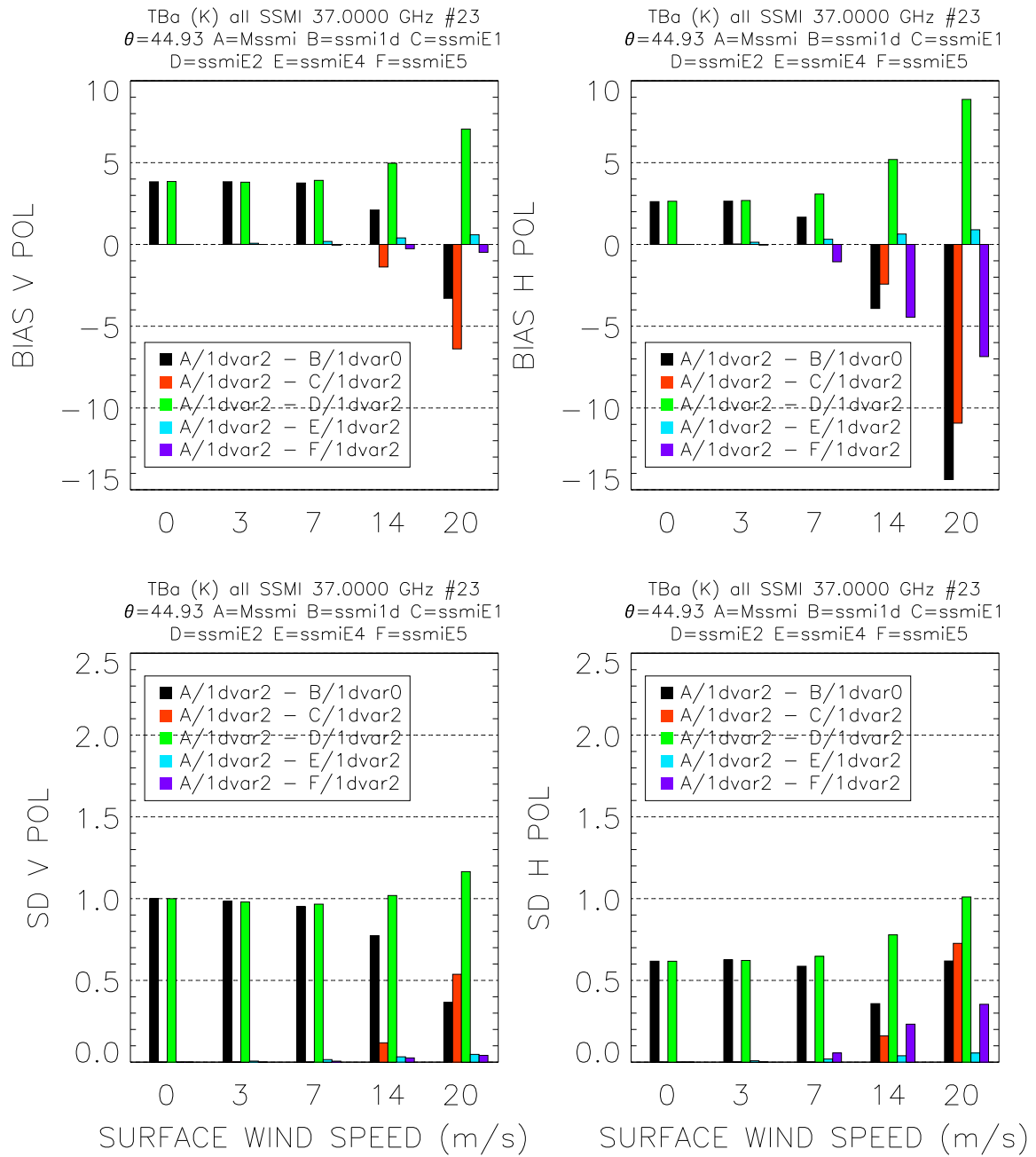Figure 4b: Same as Figure 4a but for the SSM/I frequency of 22.235 GHz.

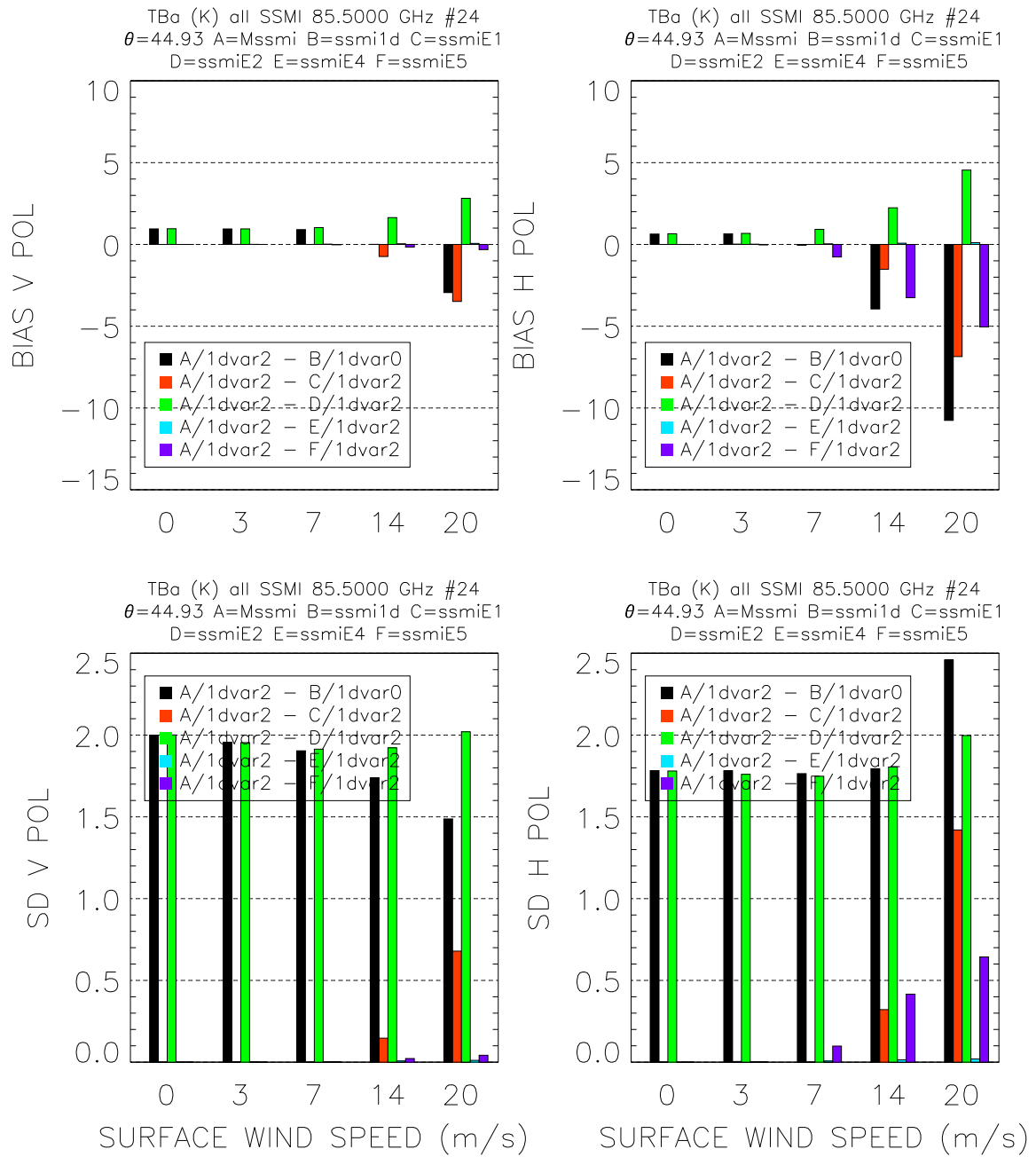Figure 4c: Same as Figure 4a but for the SSM/I frequency of 37.0 GHz.

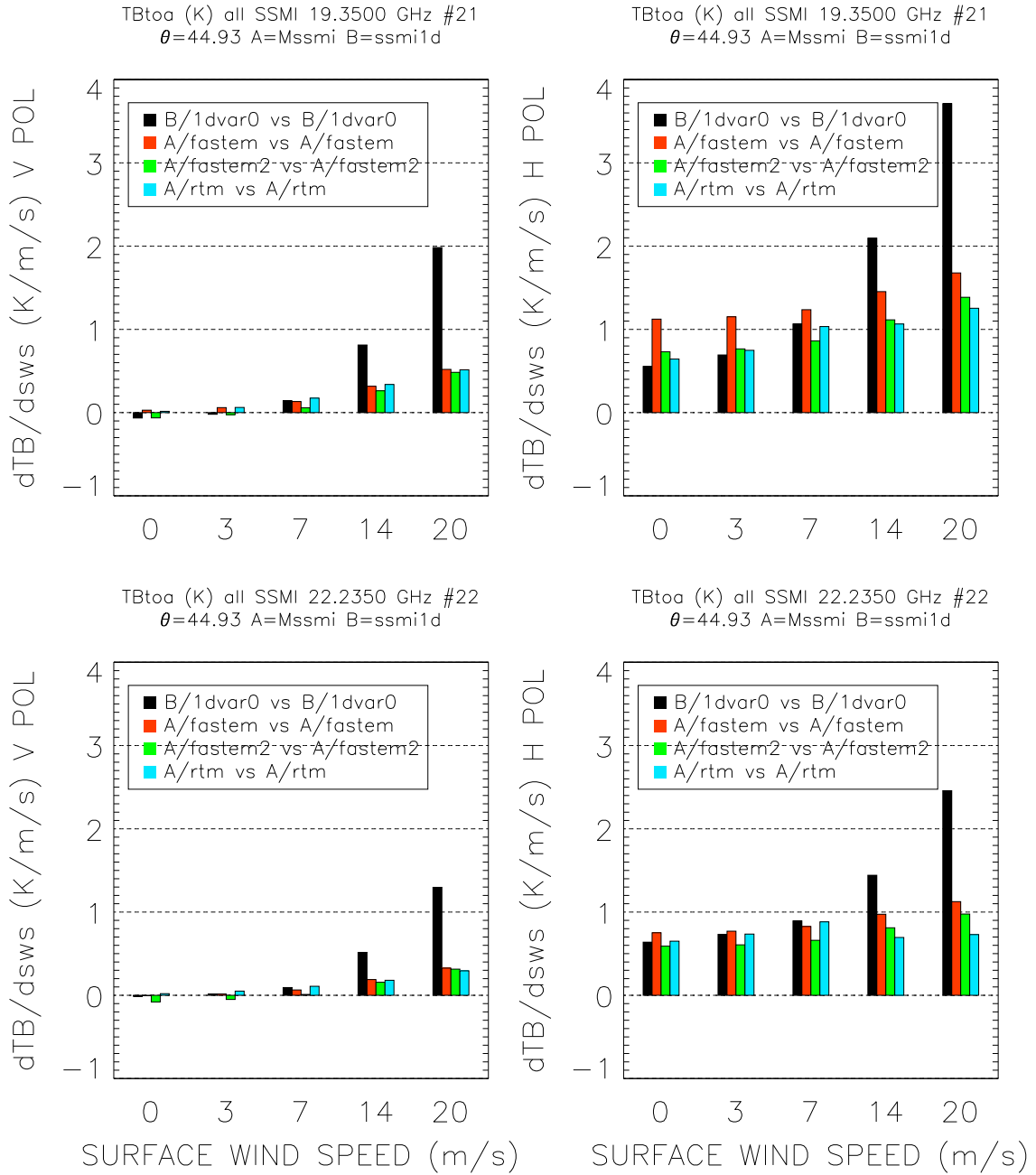Figure 4d: Same as Figure 4a but for the SSM/I frequency of 85.5 GHz.

Figure 5a: Sensitivity of the brightness temperature at the top of the atmosphere to surface wind speed ( ) for the SSM/I 19.35 and 22.235 GHz channel as a function of surface wind speed and for the 4 following models (there are 4 bars for each wind speed): (1) 1dvar0, (2) fastem, (3) fastem2 and (4) rtm. The sensitivity was averaged over all profiles of the GARAND26 data set.
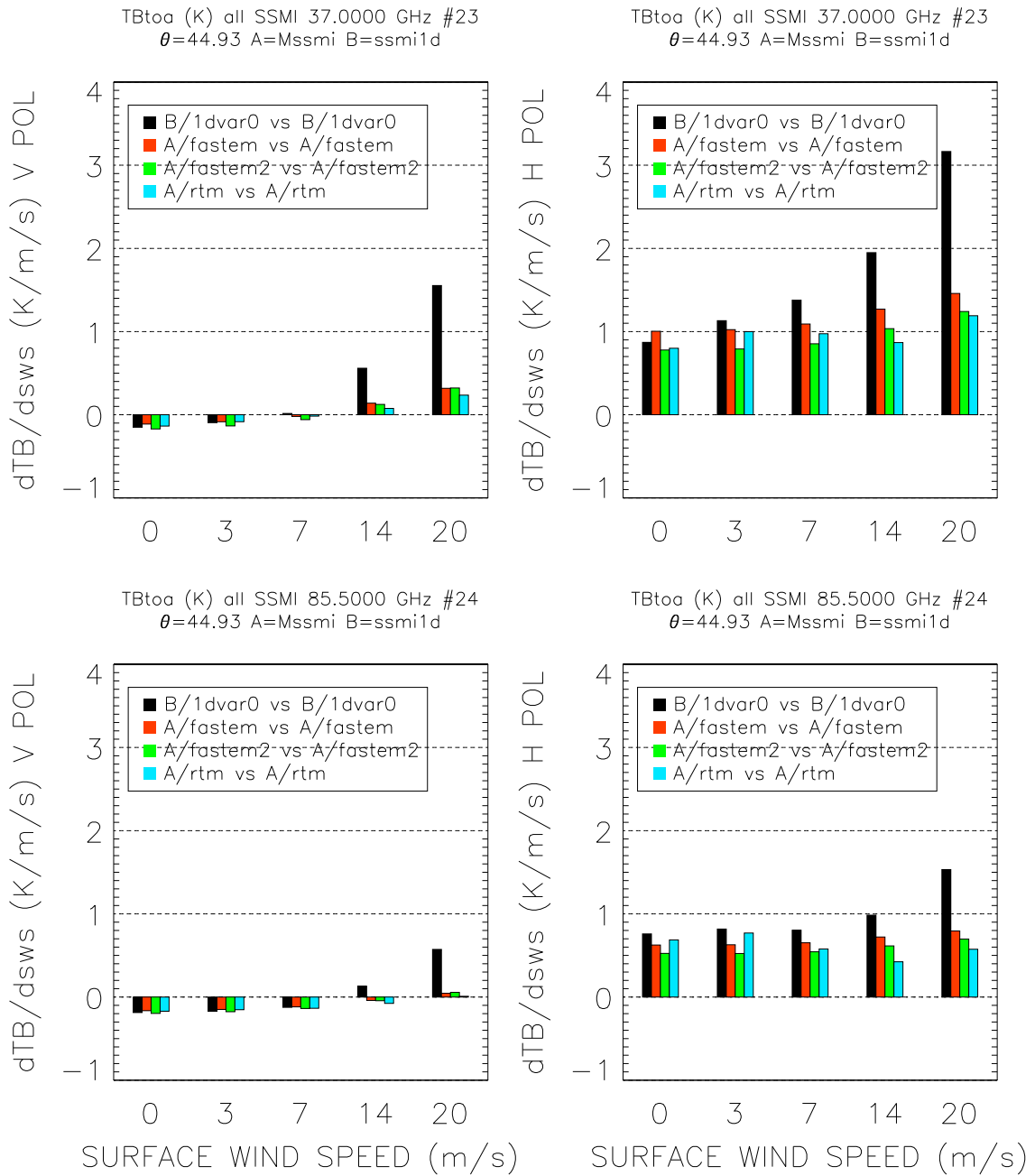
44

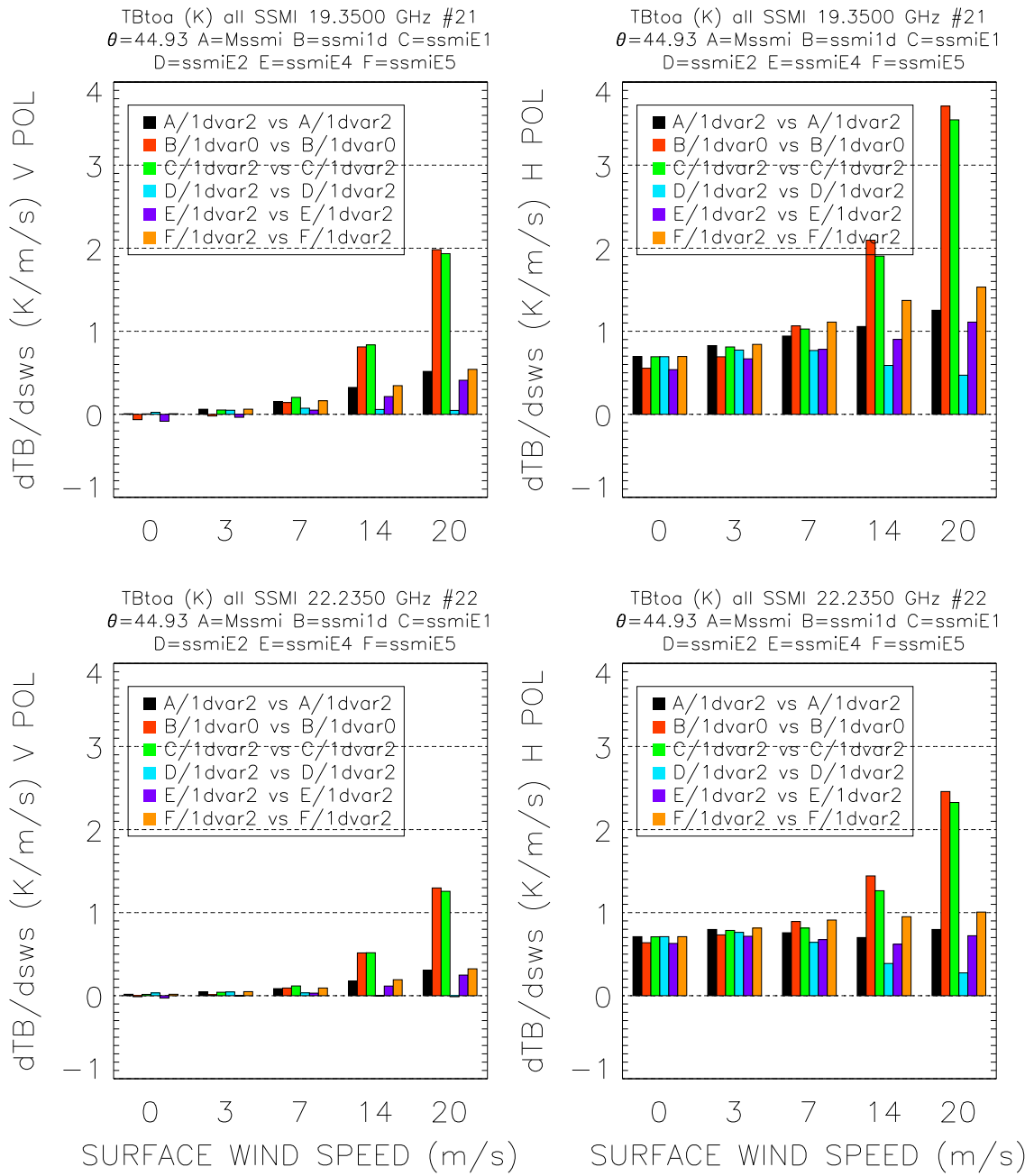Figure 5b: as in Figure 5a but for the SSM/I frequencies 37.00 and 85.5 GHz.

_

Figure 6a: Sensitivity of the brightness temperature at the top of the atmosphere to surface wind speed ($\frac{dTB}{dSWS}$) for the SSM/I 19.35 and 22.235 GHz channel as a function of surface wind speed and for the 6 following models (there are 6 bars for each wind speed): (1) 1dvar2 (#1, rtm setup), (2) 1dvar0, (3) 1dvar2 (#4)—foam change, (4) 1dvar2 (#5)—dielectric constant change, (5) 1dvar2 (#6)—Bragg scattering change and (6) 1dvar2 (#3)—multiple reflection change. The sensitivity was averaged over all profiles of the GARAND26 data set.
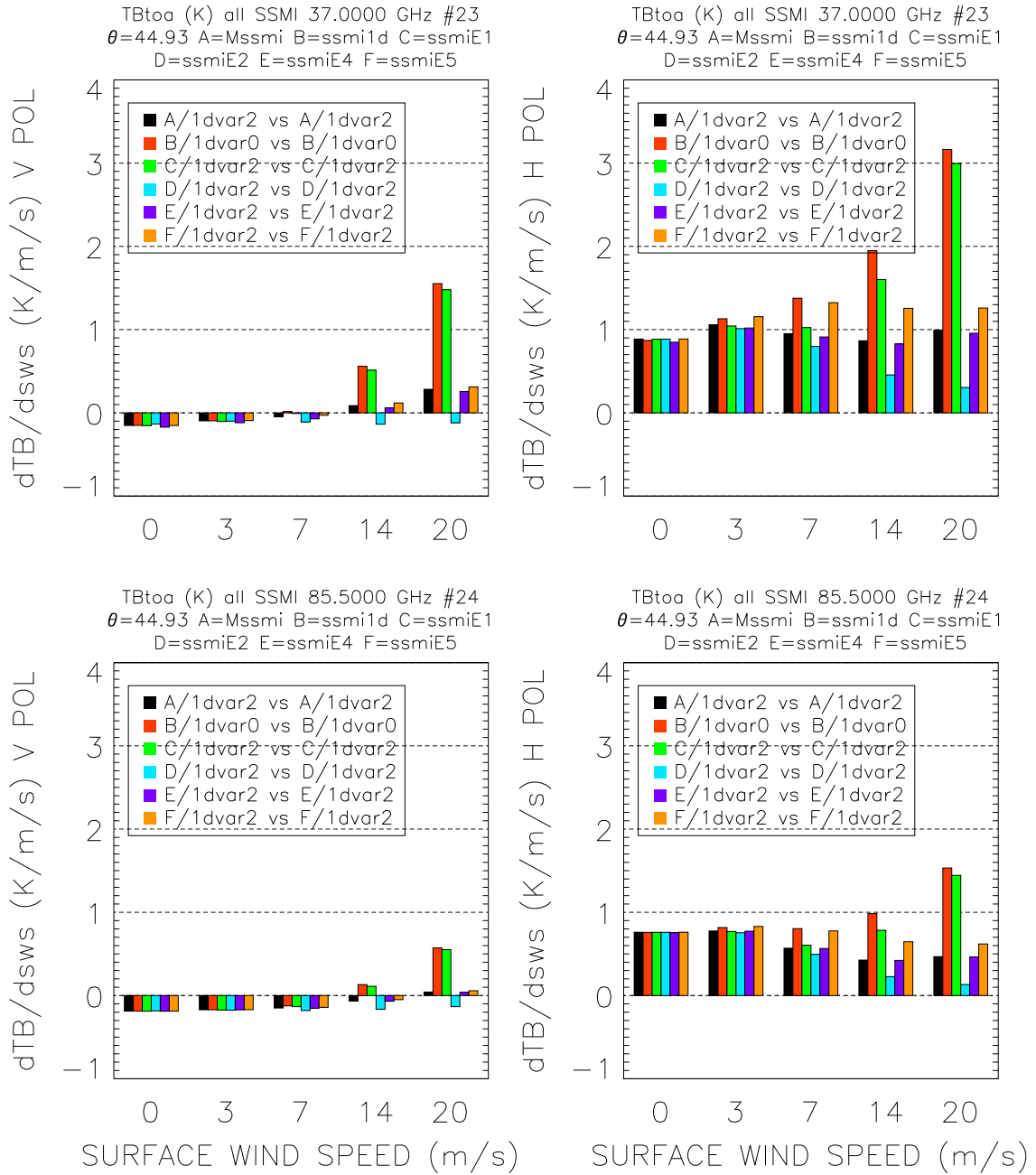
Figure 6b: Same as in Figure 6a but for the SSM/I 37.00 and 85.5 GHz channels.

COMPUTED APPARENT SURFACE TEMPERATURE (K)

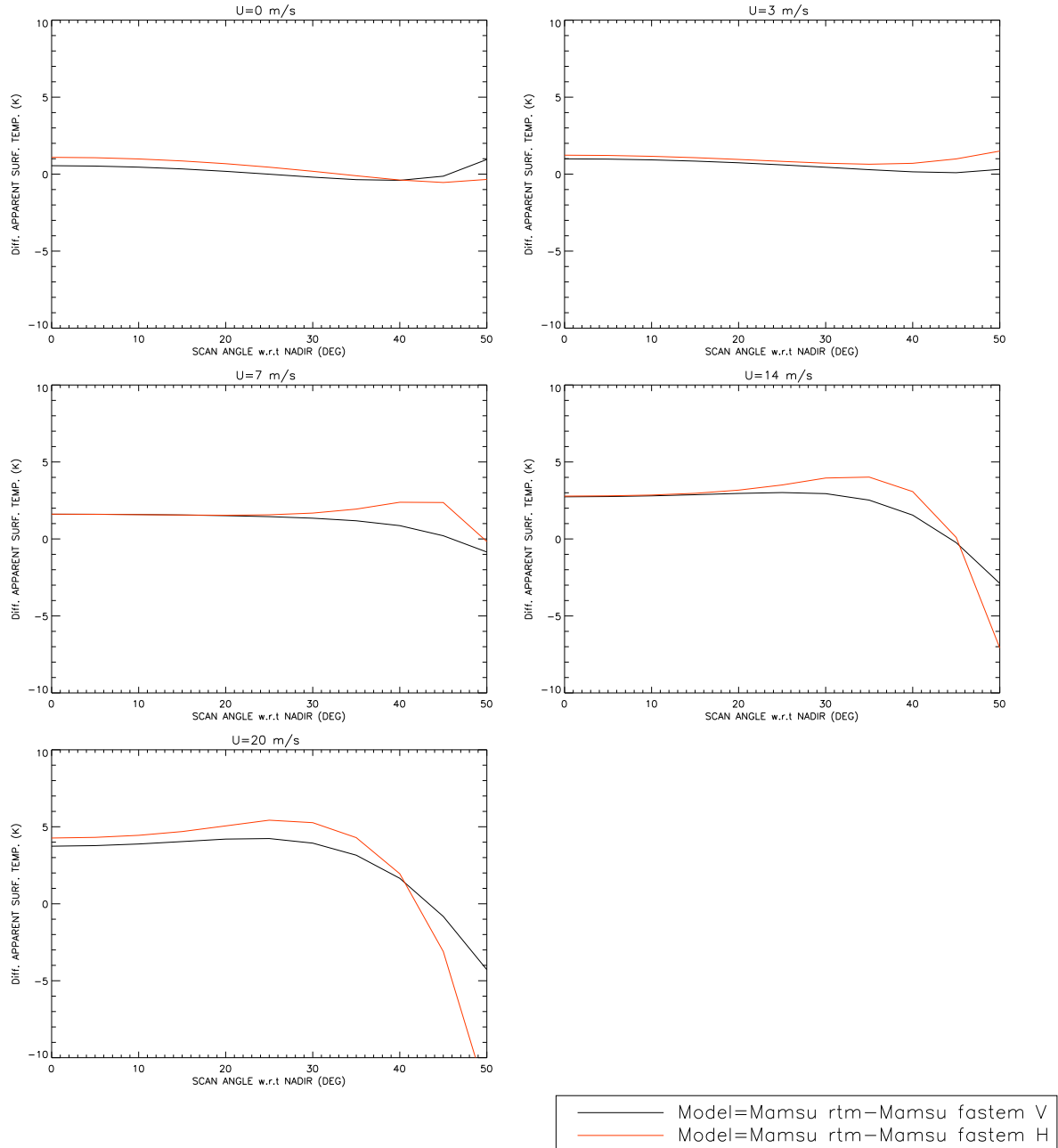Frequency=50.3000 GHz #3 TPW=33 kg/m**2

Figure 7a: Differences in apparent surface temperature as a function of scan angle for the AMSU channel 3 (50.3 GHz) for a profile with a TPW of 33 kgm^{-2}. Five plots are presented each for a different surface wind speeds (0, 3, 7, 14 and 20 ms^{-1}). Differences are computed between the models rtm and fastem. The differences for both polarizations are also presented See legend).

COMPUTED APPARENT SURFACE TEMPERATURE (K)
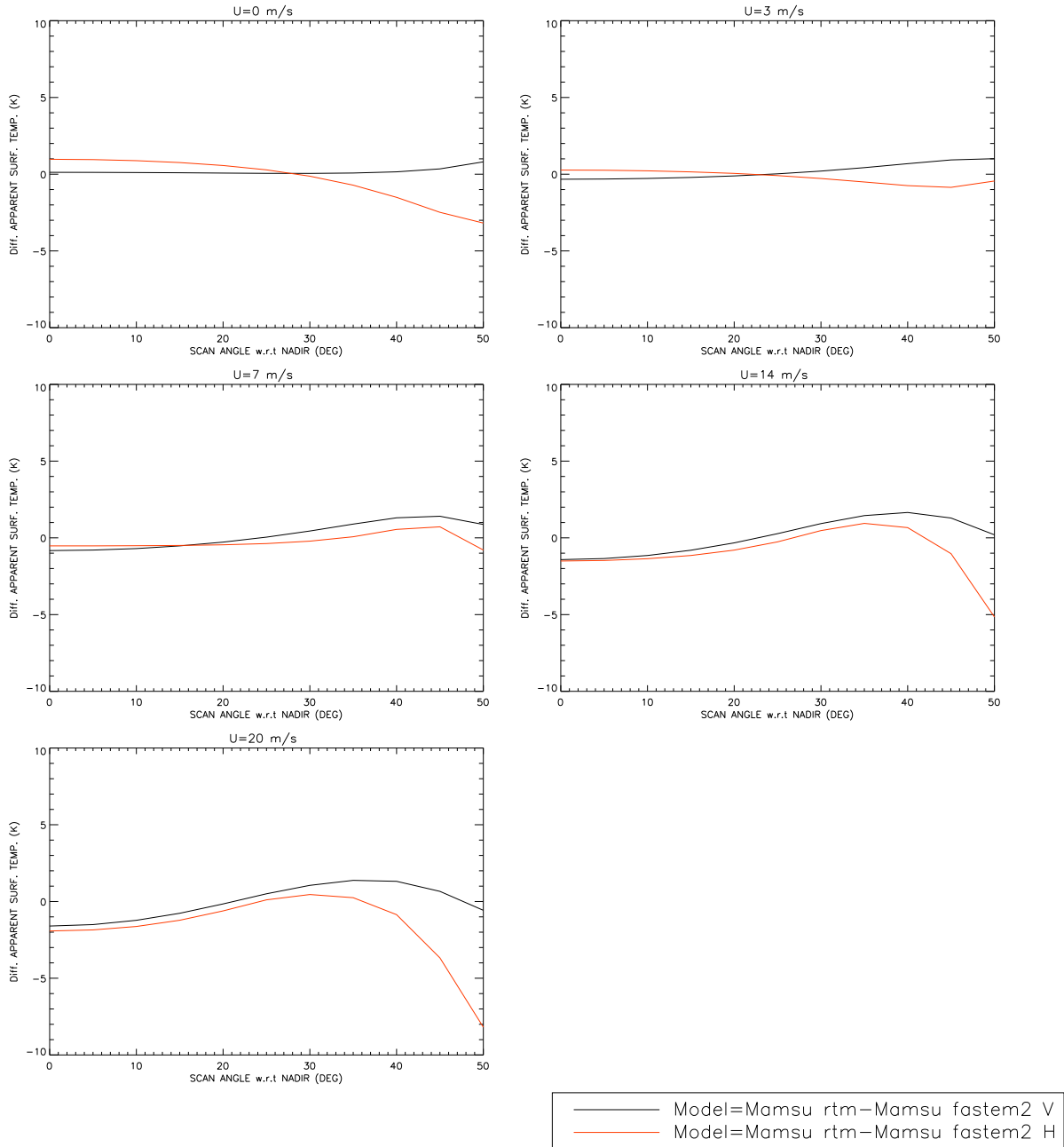
Frequency=50.3000 GHz #3 TPW=33 kg/m**2

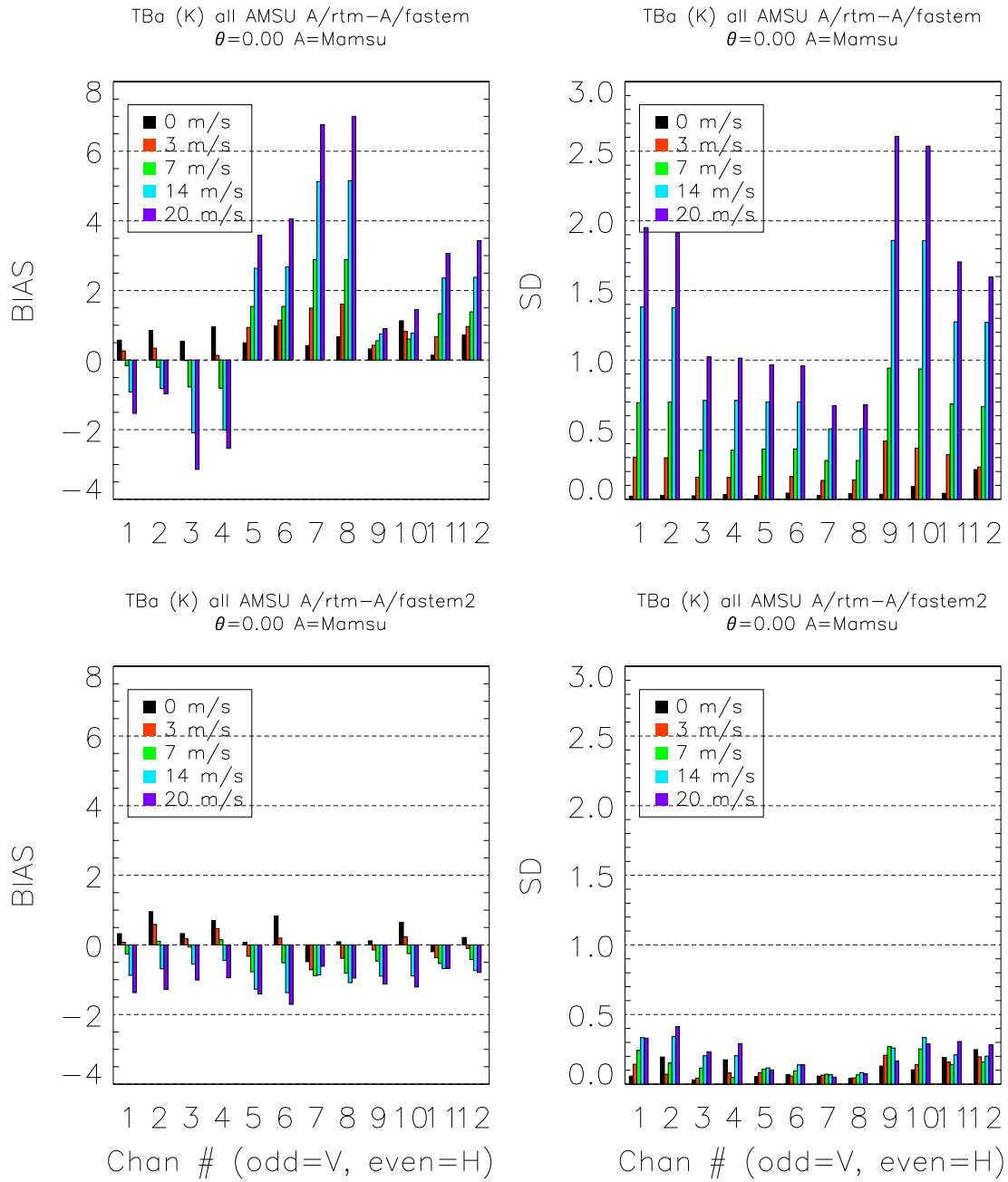Figure 7b: Same as Figure 7a but the differences are computed between models rtm and fastem2

Figure 7c: Bias and SD of the apparent surface temperature for the models rtm and fastem (top bar plots) and rtm and fastem2 (bottom bar plots) for the GARAND26 profile data set and for a scan angle of 0°. The AMSU channels are defined as follows (in GHz): (1) 23.8 V, (2) 23.8 H, (3) 31.4 V, (4) 31.4 H, (5) 50.3 V, (6) 50.3 H, (7) 52.8V, (8) 52.8 H, (9) 89 V, (10) 89 H, (11) 150.0 V, (12) 150.0 H.
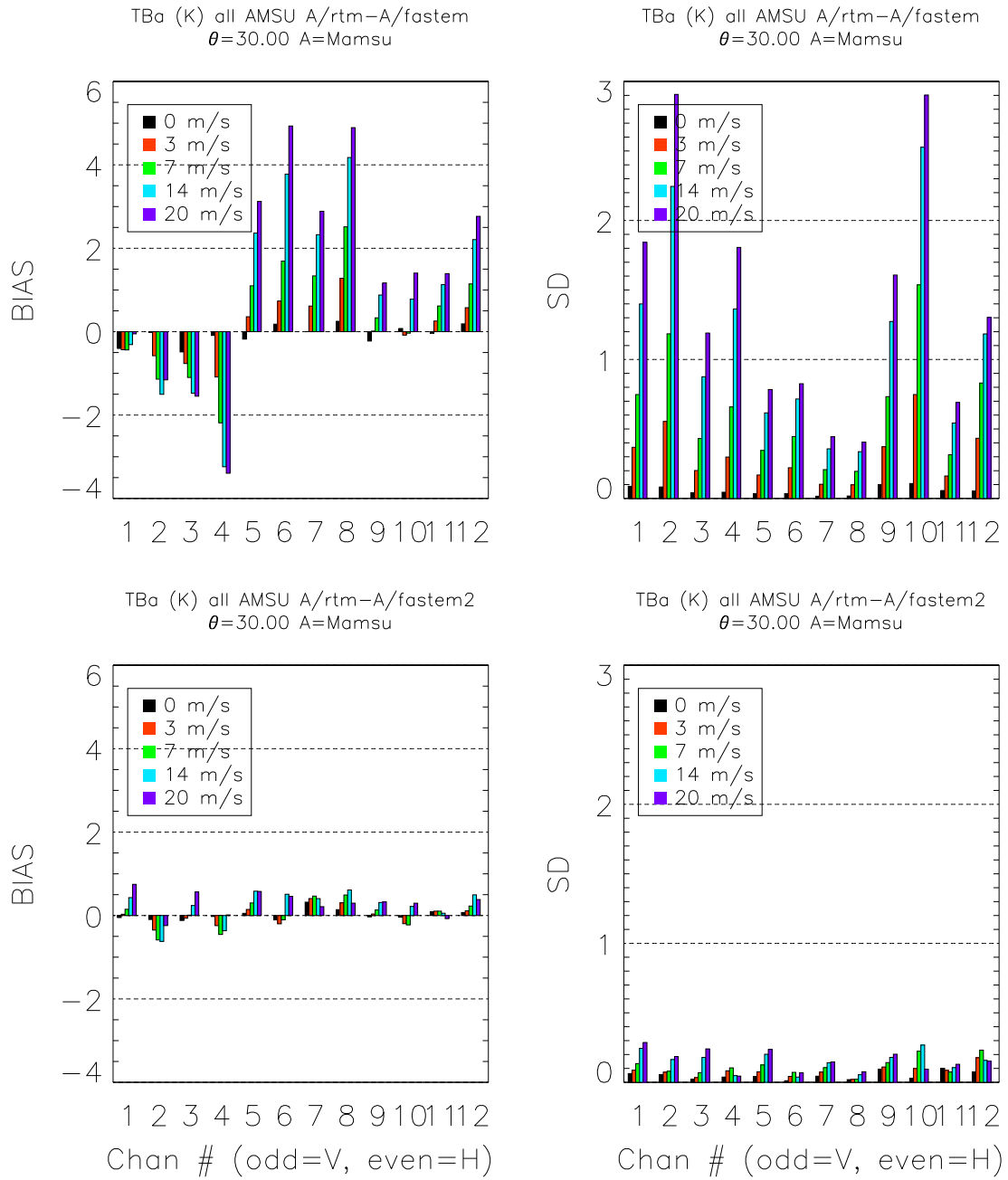
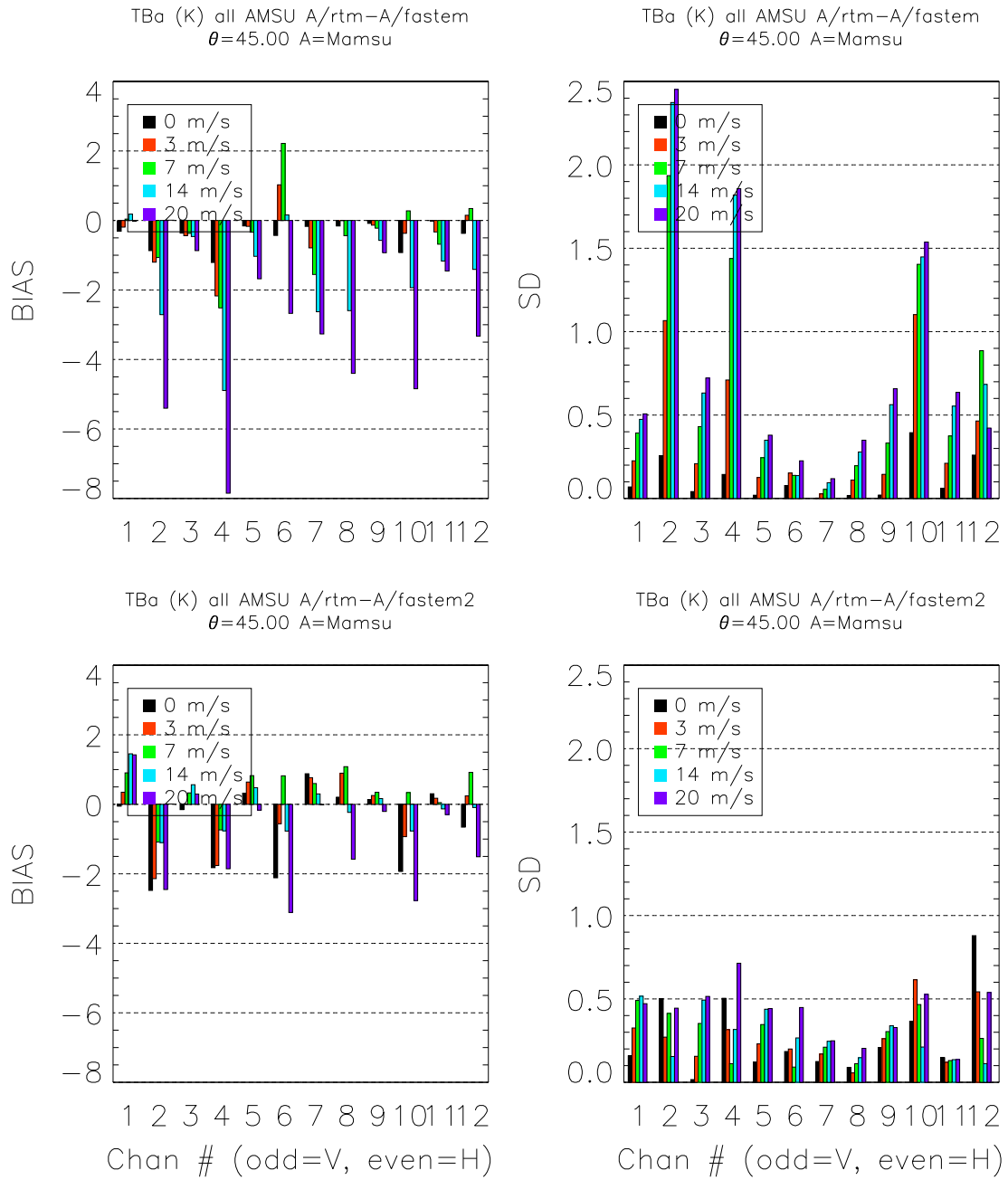Figure 7d: same as in Figure 7c but for a scan angle of 30°.

Figure 7e: same as in Figure 7c but for a scan angle of 45°.

Evaluation of fastem and fastem2, G. Deblonde, Nov 16, 2000, Final Version

COMPUTED APPARENT SURFACE TEMPERATURE (K)
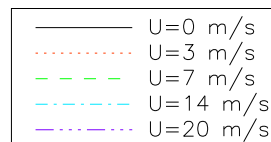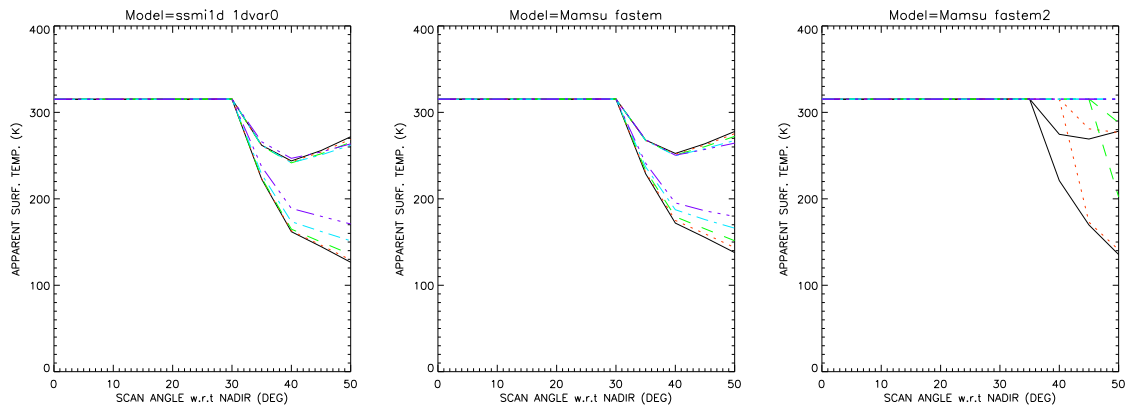
Frequency=183.310 GHz #19 TPW=33 kg/m**2

Figure 8: Illustration of the breakdown of the isothermal atmosphere approximation. The apparent surface temperature is plotted as a function of scan angle for AMSU channel 19 (183 ±3 GHz) and for a profile with a TPW of 33 kgm^{-2}. From left to right, the models used are: 1DVAR0, FASTEM, FASTEM2. The top set of curves are for the vertical polarizations at 5 different wind speeds (0, 3, 7, 14 and 20 ms^{-1}) and the bottom curves are for the horizontal polarizations and the same wind speed.